

HEAT TRANSFER UNDER A PULSED SLOT TURBULENT IMPINGING JET AT LARGE TEMPERATURE DIFFERENCES

by

Peng XU^{a*}, **Arun S. MUJUMDAR**^b, **Hee Joo POH**^c, and **Boming YU**^d

^a Institute of Surface Physics, College of Science, China Jiliang University, Hangzhou, P. R. China

^b Department of Mechanical Engineering, National University of Singapore, Singapore

^c Fluid Dynamics Division, Institute of High Performance Computing, Singapore

^d School of Physics, Huazhong University of Science and Tehnology, Wuhan, P. R. China

Original scientific paper
UDC: 536.25:662.98
DOI: 10.2289/TSCI1001271X

Pulsed impinging jets have received increasing interest for their potential in heat and mass transfer enhancement. However, published results on effects of pulsations under different flow and geometrical parameters have shown conflicting results. To further understand the flow and thermal processes in pulsed impinging jets, a numerical investigation has been performed on a two dimensional pulsed turbulent impinging jet under large temperature differences between the jet flow and the impinging surface to examine the effect of temperature-dependent thermophysical properties along with pulsation of the jet on the local Nusselt number distribution on the target surface. The numerical results show that the local time-averaged Nusselt numbers calculated with various thermal property values at the jet, film and impingement surface temperatures differ significantly for large temperature difference cases (>100 K). A parametric study for both heating and cooling cases indicates that no obvious enhancement by single sinusoidal pulsation can be found under current conditions except for cases with large temperature differences at distances far from stagnation point, i. e. in the wall jet region.

Key words: *pulsed impinging jet, sinusoidal pulsation, heat transfer, Nusselt number*

Introduction

Jet impingement has been commonly used in a great number of major industrial areas for various cooling, heating, and drying purposes due to their high convective heat transfer coefficients. Its industrial applications include thermal drying of continuous sheets of materials (*e. g.*, textiles, films, papers, veneer, lumber, *etc.*) and foodstuff productions, electronic component and gas turbine cooling, manufacture of printed wiring boards and metal sheet, printing processes, deicing or aircraft wings and tempering of glass and non-ferrous metal sheets. Over the past several decades, extensive studies have been conducted on heat and mass transfer characteristics in impinging jets [1-4]. Previous studies have mainly focused on optimizing transport

* Corresponding author; e-mail: xupenghust@yahoo.com.cn

processes associated with *steady* impinging jets. Recently, *pulsed* impinging jets have received increasing interests as flow pulsation is widely believed to increase heat transfer [5-24]. However, the existing investigations on the influence of pulsations on heat transfer under different flow and geometrical parameters show conflicting results. Both enhancement and no enhancement have been reported. Further studies are therefore warranted.

Many investigators have reported significant enhancement of heat transfer in pulsed impinging jets considering the possible features induced by the pulsations such as higher turbulence promoted by flow instabilities, increased entrainment by larger vortices, and non-linear dynamic response of the hydrodynamic and thermal boundary layers *etc.* [5-13]. Kataoka *et al.* indicated that the stagnation point heat transfer for axisymmetric submerged jets was enhanced by impingement of large-scale structures [5]. Zumbrunne *et al.* have reported a twofold enhancement of heat transfer in a planar impinging water jet with pulsation frequency in order of 100 Hz [6]. The experimental work shows that the enhancement depends on Reynolds number, impingement height, frequency, and amplitude of pulsations [6, 8, 9]. The tests by Sailor *et al.* show that the duty cycle representing the ration of pulse cycle on time to total cycle time has a significant effect on the heat transfer enhancement in an impinging air jet [10]. Camci *et al.* found strong increases in heat transfer at very large nozzle-to-plate distance ($H/w = 24\sim 60$) and Reynolds numbers of 7500-14000 [11]. The measurements of heat transfer in circular air jet by Zulkifli *et al.* show that the stagnation point heat transfer doesn't show any enhancement but the local heat transfer away from the stagnation point is significant enhanced for the higher turbulence intensity in this region [12, 13].

Some investigators only found a marginally beneficial effect of pulsation on heat transfer [14-18]. Chaniotis *et al.* numerically studied the effect of jet pulsation on heat transfer and fluid dynamics characteristics of single and double jet impingement on a constant heat flux heated surface with the smooth particle hydrodynamics methodology, they stated the improvement of pulsation in the maximum temperature is not very large [15]. Behera *et al.* investigated the effect of sinusoidal- and square-wave pulsations on heat transfer by computational fluid dynamic (CFD), and show that the augmentation of the sinusoidal-wave pulsation which is less than 10% takes effect only for large amplitudes (>40%) [16]. The numerical results of Poh *et al.* on a 2-D planar impinging jet show that the heat transfer performance enhancement of both of laminar and turbulent pulsations is marginal [17, 18].

While many investigations indicate no enhancement of heat transfer or even show some deterioration of heat transfer as the pulsation energy mainly contributes to mixing between the jet and environment [19-24]. Fallen found no influence of pulsation on heat transfer in laminar flow, and only a slight increase or decrease in turbulent flow depending on frequency [19]. The experiments on cooling performance with an impinging water jet by Sheriff *et al.* where both of sinusoidal and square-pulse waveforms were used indicate that the reductions of local heat transfer by the sinusoidal pulsation decrease markedly from the stagnation point [20]. The investigation of Azevedo *et al.* on jet impingement with a rotating cylinder valve for a range of pulse frequency show that heat transfer degraded for all frequencies [21]. Mladin *et al.* reported a negligible increase (1%) in heat transfer in case of low amplitude and high frequencies and a decrease of heat transfer by the pulsation of up to 17% over a large range of frequencies, and they argued that high pulse frequency and low amplitude are better than low frequency and high amplitude [22, 23]. The examinations of axisymmetric impinging jets by Vejrazka also show no influence of pulsation on heat transfer [24].

Several researchers presented threshold values for effective pulsed impinging jet heat transfer [25, 26]. Mladin *et al.* reported a threshold Strouhal number (0.26), below which no significant heat transfer enhancement is obtained [25]. However, Sailor *et al.* still found significant enhancement in the stagnation point heat transfer for pulse flow at Strouhal number between 0.009 and 0.042 [10]. Recently, Hoffmann *et al.* investigated the influence of a pulsation on flow structure and heat transfer with experiments, and determined the threshold Strouhal number for small nozzle-to-plate distances to be in order of 0.2 [26].

Because of the complexity of flow structures and the non-linear dynamics in the boundary layer induced by pulsation, pulsed jet impingement flow and associated heat transfer has been a challenging problem and shown some intriguing aspects. The related physics for the pulsed jet impingement is not yet well-understood. Thus, the objective of this current study is to examine the influence of the sinusoidal pulsation on the heat and mass transfer in impinging jet by CFD method. The effect of Reynolds numbers and frequency as well as amplitude of the sinusoidal pulsation, temperature differences, and geometrical configuration will be discussed for further understanding of flow and thermal characteristics in pulsed impinging jet.

Mathematical model

As shown in fig. 1, a two dimensional symmetric slot impinging jet configuration will be numerically modeled. Due to geometric and flow symmetry, only the flow field within the half domain is solved. The fluid (air) was assumed to be incompressible and Newtonian with temperature-dependent fluid properties, and the viscous forces were negligible. Numerical simulation of the flow and thermal fields in a semi-confined turbulent impinging jet requires the solution of the continuity, eq. (1), the Navier-Stokes, eq. (2), and the energy eq. (3):

$$\frac{\partial u_i}{\partial x_i} = 0 \quad (1)$$

$$\frac{\partial(\rho u_i)}{\partial t} + \frac{\partial(\rho u_i u_j)}{\partial x_j} = -\frac{\partial p}{\partial x_i} + \frac{\partial}{\partial x_j} \left[\mu \left(\frac{\partial u_i}{\partial x_j} + \frac{\partial u_j}{\partial x_i} \right) - \rho \overline{u'_i u'_j} \right] + \rho g_i \quad (2)$$

$$\rho c_p \left[\frac{\partial T}{\partial t} + \frac{\partial(u_j T)}{\partial x_j} \right] = \frac{\partial}{\partial x_j} \left(k \frac{\partial T}{\partial x_j} - \rho c_p \overline{u'_j T'} \right) \quad (3)$$

The Reynolds number based on the mean jet exit velocity u_{jet} and slot width w is $Re = \rho u_{jet} w / \mu$. Many different turbulence models *e. g.* $k-\epsilon$, $k-\omega$, Reynolds stress, and v^2f model were used to model turbulent flow in *steady* impinging jets. The $k-\epsilon$ model can only present reasonable agreement with experimental data for certain cases, as it cannot handle rapid length scale change and strong streamline curvature in the stagnation area, which can cause an anomalous turbulence production and lead to over-prediction of the heat transfer [27]. The $k-\omega$ model has received attention in modeling turbulent impingement flows as it is easy to implement and often

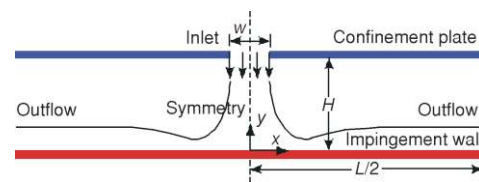


Figure 1. Physical model of the single pulsed slot impinging jet simulated (color image see on our web site)

predicts better results compared to those using the $k-\varepsilon$ model [28]. The Reynolds stress model (RSM), taking anisotropy of the turbulence in the near-wall region account, has been shown to be superior to those $k-\varepsilon$ and $k-\omega$ models [29, 30]. The v^2f model has also been indicated good agreement with a wide range of experimental results [31]. However, the v^2f model is more expensive as it requires resolution all the way to the wall without wall function approximation. In the present study, these four turbulence models will be firstly tested for *sinusoidal pulsed* turbulent impinging jet.

The following boundary conditions were used. A sinusoidal pulsation with flat velocity profile was applied at the inlet of the impinging jet as described below:

$$u_{\text{jet}} = u_{\text{avg}} + Au_{\text{avg}} \sin(2\pi ft) \quad (4)$$

The jet flow and impingement surface were specified as isothermal, and the confinement wall was considered to be adiabatic; the uniform velocity, temperature, turbulent kinetic energy and energy dissipation rate profiles were assumed at the nozzle exit; no-slip condition was imposed at the impingement wall; the symmetry and fully developed outflow boundary conditions were taken at symmetry and outlet planes. The initial conditions ($t = 0$) throughout the computational domain can be described as: $u = v = 0$, $p = p_{\infty}$, and $T = T_{\infty}$. The finite volume

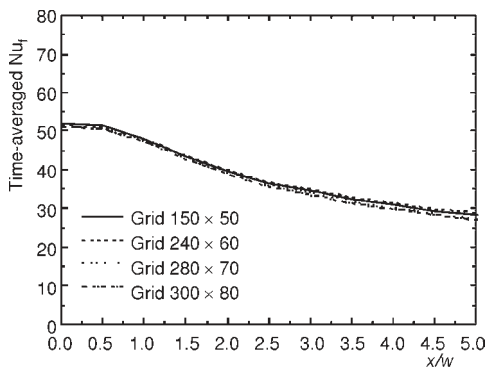


Figure 2. Effect of grid density on the time-averaged Nusselt number distribution
($H/w = 5$, $Re = 11,000$, $\Delta T = 100$ K, $A = 50\%$, $f = 60$ Hz)

CFD code FLUENT 6.3 was used to numerically solve the flow and thermal fields in the pulsed turbulent impingement jet on a two dimensional symmetry domain. As the near-wall treatment is important in situations with heat and mass transfer near solid surfaces, thus, the boundary layer near the surface was kept in the order of $y^+ \approx 1$. Grid-independence of the final results was checked with different grid densities. Figure 2 shows the effect of grid size on the predicted time-averaged Nusselt number distribution. Typically, a grid density of 150×50 provides satisfactory solution for the example shown. A second upwind discretization scheme was used considering the stability of solution convergence and the SIMPLEC algorithm was employed for the pressure-velocity coupling.

Results and discussion

The local Nusselt number for an isothermal impingement surface is conventionally defined as:

$$\text{Nu} = \frac{q}{T_j - T_s} \frac{w}{k(T)} \quad (5)$$

The thermal conductivity of jet fluid k can be calculated according to different reference temperatures. Generally, the fluid conductivity calculated at jet temperature T_j , film temperature $T_f = (T_j + T_s)/2$ and impingement surface temperature T_s , and the corresponding Nusselt numbers are denoted by Nu_j , Nu_f , and Nu_s , respectively. The Nusselt number varies with time

and position, therefore, the time-averaged local Nusselt number and time-averaged total Nusselt number can be, respectively, calculated by:

$$\text{Nu}_{\text{avg}}(x) = \int_0^t \frac{1}{\Delta t} \text{Nu}(x, t) dt \quad (6a)$$

$$\text{Nu}_{\text{avg}} = \int_0^x \frac{1}{\Delta x} \int_0^t \frac{1}{\Delta t} \text{Nu}(x, t) dt dx \quad (6b)$$

So far, most studies have involved small temperature differences between that of jet flow and target surface. Under small temperature differences, all fluid properties can be regarded as temperature-independent and the differences between the local Nusselt numbers calculated with thermal conductivity values at the jet, film, and impingement surface can be neglected. However, in some industrial applications such as fast paper drying and turbine blade cooling, very high temperature and large temperature difference which involve temperature-dependent thermophysical properties are used to obtain very high heat transfer rates. The study of Shi *et al.* on steady turbulent slot impingement jet involving temperature differences ranging from 12 to 272 °C indicates that large temperature differences lead to significant differences in the heat transfer coefficients [32]. It is therefore necessary to compare local Nusselt number with the three definitions in pulsed impinging jet under large temperature differences.

Model validation

Since few investigations have been conducted on the predictive ability of various turbulence models for pulsed turbulent impinging jets, four turbulence models frequently used for steady turbulent impinging jets: standard $k-\varepsilon$ model, $k-\omega$ model, RSM, and v^2f model were tested for sinusoidal pulsed turbulent impinging jet for a cooling application. The time-averaged Nusselt number calculated at the film temperature Nu_f was used to validate present mathematical models; the film temperature is usually adopted in experimental calculations [9]. Figure 3(a) shows a comparison between the numerically predicted local time-averaged Nusselt number Nu_f distributions and that of pulsed and steady impinging jet experi-

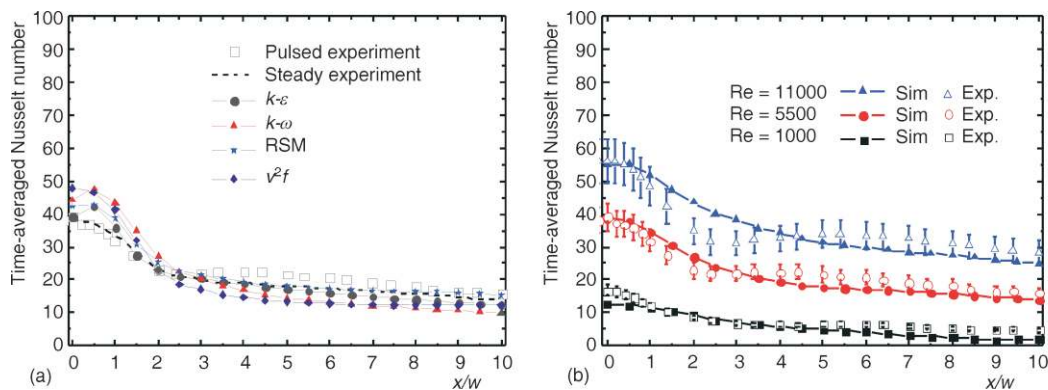


Figure 3. Comparison of numerical results with experimental results [9] at $H/w = 5$
 (a) turbulence model test at $H/w = 5$, $Re = 5500$, $A = 17\%$, and $f = 41$ Hz; (b) predicted Nusselt number distribution with RSM at $Re = 1000$ ($A = 12\%$, $f = 23$ Hz), 5500 ($A = 17\%$, $f = 41$ Hz), and 11000 ($A = 25\%$, $f = 41$ Hz) (color image see on our web site)

ments for $H/w = 5$ and $Re = 5500$. It can be seen that the RSM predicts better local Nusselt number distribution at amplitude $A = 17\%$ and frequency $f = 41$ Hz. Figure 3(b) shows a comparison between the numerically predicted time-averaged Nusselt number Nu_f distributions by RSM with that of pulsed impinging jet experiments under $H/w = 5$ and $Re = 1000, 5500,$ and 11000 . Considering the relatively large relative error of the experiments (9.6%, 10.6%, and 12% for $Re = 1000, 5500,$ and 11000 , respectively), the RSM can capture the overall shape of the Nusselt number distribution relatively well. The RSM model can make reasonable prediction near the stagnation point but slightly overestimates the magnitudes of Nusselt number in the wall jet region. Thus, this model is therefore deemed acceptable for subsequent simulation runs.

Parametric study for cooling case

For the cooling case, the temperature of jet flow is set as T_∞ , and the temperature differences between the jet flow and that of impinging surface range from 50 to 400 K. The effects of Reynolds number ranging from 5500 to 25000, frequency from 20 to 80 Hz and amplitude from 5 to 50% as well the nozzle-to-plate distance ranging from 3 to 8 are discussed for further understanding of the flow and thermal characteristics in pulsed turbulent impinging jets under large temperature differences and to examine the effect of pulsation on heat transfer.

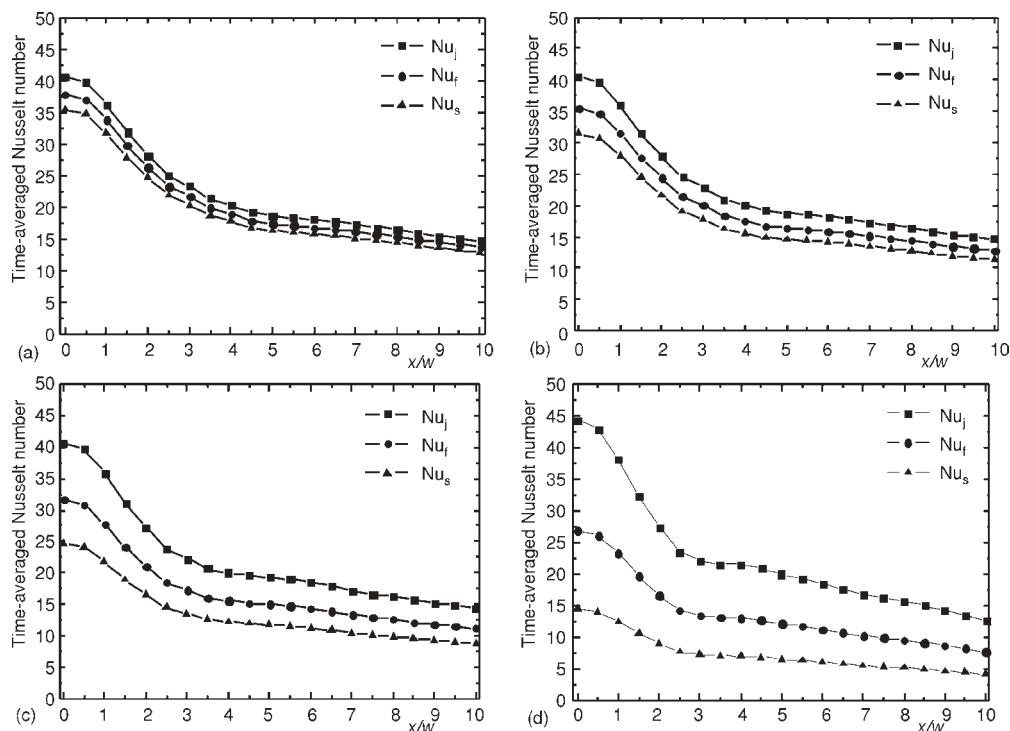


Figure 4. Local Nusselt number distributions under $H/w = 5$, $Re = 5500$, $A = 17\%$, and $f = 41$ Hz with different reference temperature (color image see on our web site)
(a) $\Delta T = 50$ K, (b) $\Delta T = 100$ K, (c) $\Delta T = 200$ K, and (d) $\Delta T = 400$ K

Figure 4 indicates three possible local Nusselt numbers at large temperature differences between impinging jet and impingement surface of $\Delta T = 50$ K, $\Delta T = 100$ K, $\Delta T = 200$ K, and $\Delta T = 400$ K, respectively. In the cooling case, as the jet flow temperature is lower than that of the impingement surface, the time-averaged Nusselt number with jet temperature is larger than that with film temperature which is larger than that with impingement surface temperature, $Nu_j > Nu_f > Nu_s$. At a low temperature difference, $\Delta T = 50$ K, the three time-averaged Nusselt numbers are as expected close to each other and the maximum difference between Nu_j and Nu_s is within 10% which can be approximately neglected, fig. 4(a). However, the difference between the three Nusselt numbers increases as the temperature difference increases. For example, at large temperature difference $\Delta T = 400$ K, Nu_j is even two times larger than Nu_s . Figure 5 shows the distributions of local time-averaged Nusselt number at film temperature under various temperature differences between the jet flow and impingement surface. It is clear that the larger of the temperature difference, the smaller of the time-averaged Nusselt number. Negligible difference between pulsed and steady impinging jet is obtained even at large temperature difference.

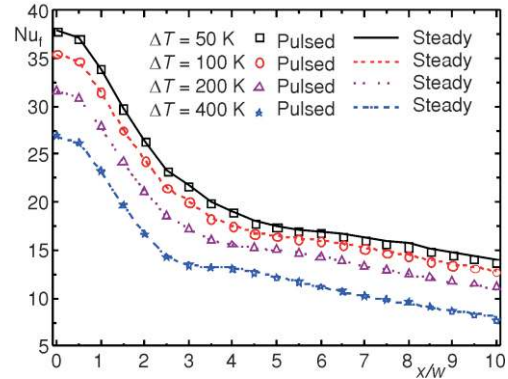


Figure 5. Effect of temperature difference on time-averaged local Nusselt number at $H/w = 5$, $Re = 5500$, $A = 17\%$, and $f = 41$ Hz (color image see on our web site)

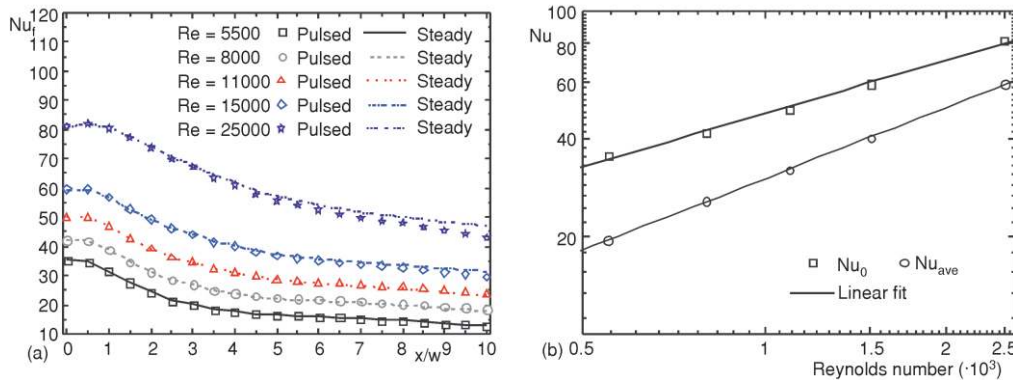


Figure 6. (a) Local time-averaged Nusselt number distribution; (b) Correlation between Nusselt number and Reynolds number ($H/w = 5$, $\Delta T = 100$ K, $A = 17\%$, $f = 41$ Hz) (color image see on our web site)

The effect of the mean jet Reynolds number on time-averaged Nusselt number is portrayed in fig. 6, where it can be observed that increasing Reynolds number enhances heat transfer in pulsed impinging jet. Under the present conditions ($H/w = 5$, $\Delta T = 100$ K, $A = 17\%$, $f = 41$ Hz) and Reynolds number ranging from 5500 to 25000, almost no enhancement on heat transfer can be found that is attributable to pulsation. Even at different amplitudes and frequencies of pulsation, the effect of pulsation on heat transfer in impinging jet is not appreciable (fig.

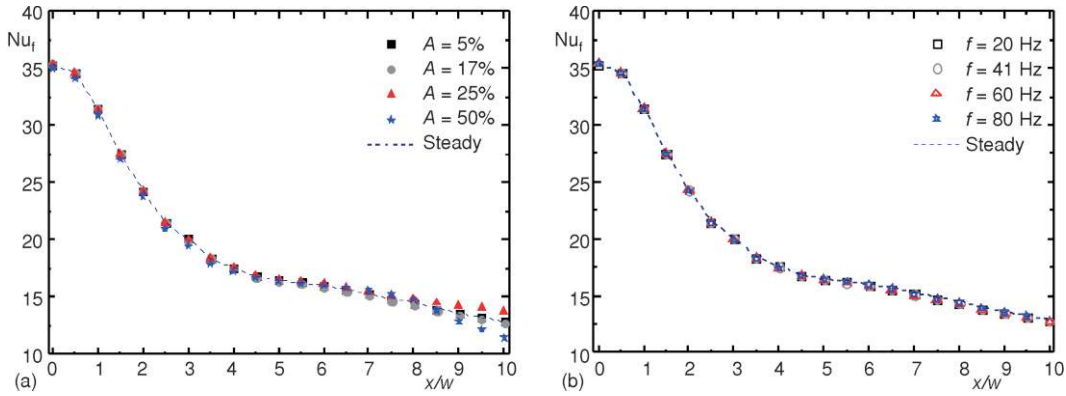


Figure 7. Effect of amplitude (a) and frequency (b) of sinusoidal pulsation on time-averaged Nusselt number distribution under $H/w = 5$, $Re = 5500$, and $\Delta T = 100$ K (color image see on our web site)

7). Figures 7(a) and (b) indicate that the effects of amplitude and frequency on the time-averaged local Nusselt number distribution are very small, even negligible. Further calculation indicates that a scaling law can be found between the time-averaged total Nusselt number and Reynolds number as $Nu_{ave} \sim Re^{0.74}$, and the time-averaged local Nusselt number at stagnation point ($x/w = 0$) relates with Reynolds number as $Nu_0 \sim Re^{0.55}$ at $H/w = 5$, and $\Delta T = 100$ K.

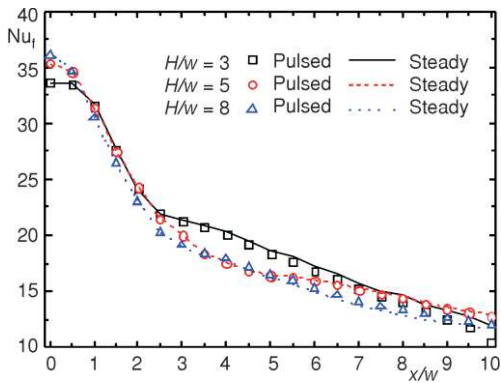


Figure 8. Effect of nozzle-to-plate distance on time-averaged Nusselt number at $\Delta T = 100$ K, $Re = 5500$, $A = 17\%$, $f = 41$ Hz, and $H/w = 3, 5$, and 8 (color image see on our web site)

Figure 8 shows the time-averaged Nusselt number distribution for various nozzle-to-plate spacings. It can be seen that the geometry of the impinging jet has important effect on its heat and mass transfer performance. It is clear from fig. 8 that the local Nusselt number near the stagnation point increases as nozzle-to-plate distance increases, which is consistent with the experimental data [9].

Figure 8 shows the time-averaged Nusselt number distribution for various nozzle-to-plate spacings. It can be seen that the geometry of the impinging jet has important effect on its heat and mass transfer performance. It is clear from fig. 8 that the local Nusselt number near the stagnation point increases as nozzle-to-plate distance increases, which is consistent with the experimental data [9].

Parametric study for heating case

The temperature of the impingement surface is taken as T_{∞} , while the jet flow temperature is much larger than that of impingement surface for heating. Numerical calculations were performed for heating cases to investigate the effect of pulsation on heat and mass transfer. The parameters considered are temperature differences ($50 \text{ K} \leq \Delta T \leq 400 \text{ K}$), mean jet Reynolds numbers ($1000 \leq Re \leq 11000$), pulsation amplitude ($5\% \leq A \leq 50\%$) and frequency ($20 \text{ Hz} \leq f \leq 60 \text{ Hz}$), as well the nozzle-to-plate distance ($3 \leq H/w \leq 10$). In the heating cases, as the jet flow temperature is larger than that of the impingement surface, Nusselt number at jet temperature is lower than that at the film temperature which is in turn smaller than that at impingement surface temperature, $Nu_j < Nu_f < Nu_s$. The numerical calculations show that reduced temperature difference and increased Reynolds number can both enhance the time-averaged local Nusselt number (fig. 9), which is similar to that observed for the cooling case. Furthermore, no evident enhancement of

The temperature of the impingement surface is taken as T_{∞} , while the jet flow temperature is

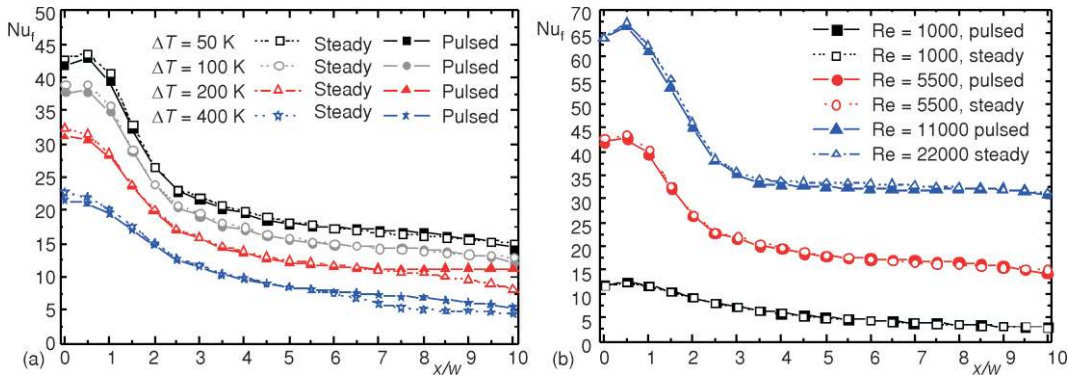


Figure 9. Effect of temperature difference (a) and Reynolds number (b) on time-averaged local Nusselt number ($H/w = 5, A = 17\%, f = 41 \text{ Hz}$) (color image see on our web site)

heat transfer by pulsation can be found for the heating case as well. At $H/w = 5$ and $\Delta T = 50 \text{ K}$, the time-averaged local Nusselt number at stagnation point ($x/w = 0$) and the time-averaged total Nusselt number show scaling laws as $Nu_0 \sim Re^{0.71}$ and $Nu_{ave} \sim Re^{0.76}$ with Reynolds number, respectively. Figure 10 shows the time-averaged Nusselt number distribution for different nozzle-to-plate spacing. It can be observed that the geometry of the impinging jet has an important effect on its heat and mass transfer. It is clear from fig. 10 that the Nusselt number decreases with increase of nozzle-to-plate distance, which is opposite to that of the cooling case.

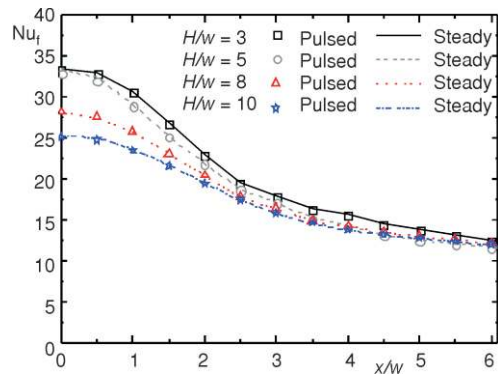


Figure 10. Effect of nozzle-to-plate distance on time-averaged Nusselt number at $\Delta T = 100 \text{ K}$, $Re = 5500, A = 17\%, f = 41 \text{ Hz}$, and $H/w = 3, 5, 8,$ and 10 (color image see on our web site)

Concluding remarks

The effects of large temperature differences, mean jet Reynolds number, frequency, and amplitude of pulsation as well as the nozzle-to-plate distance on heat transfer in impinging jet are studied for both cooling and heating applications, respectively. The numerical results show that the local time-averaged Nusselt numbers calculated with various thermal conductivity values at the jet, film, and impingement surface temperatures in both cooling and heating cases differ significantly for large temperature differences ($>100 \text{ K}$). The temperature difference and Reynolds number have significant influence on heat transfer under pulsed turbulent impinging jets. Increased temperature differences can reduce the Nusselt number, whereas increasing Reynolds number results in Nusselt number enhancement. The results indicate that the local Nusselt number at stagnation point and the averaged Nusselt number correlate with the mean jet Reynolds number with similar scaling laws. The Nusselt number increases with increase of nozzle-to-plate distance near the stagnation point in cooling case, which is opposite to

- [10] Sailor, D. J., Rohli, D. J., Fu, Q. L., Effect of Variable Duty Cycle Flow Pulsations on Heat Transfer Enhancement for an Impinging Air Jet, *International Journal of Heat and Fluid Flow*, 20 (1999), 6, pp. 574-580
- [11] Camci, C., Herr, F., Forced Convection Heat Transfer Enhancement Using a Self-Oscillating Impinging Planar Jet, *Journal of Heat Transfer*, 124 (2002), 4, pp. 770-782
- [12] Zulkifli, R., Sopian, K. K., Studies on Pulse Jet Impingement Heat Transfer: Flow Profile and Effect of Pulse Frequencies on Heat Transfer, *International Journal of Engineering and Technology*, 4 (2007), 1, pp. 86-94
- [13] Zulkifli, R., *et al.*, Comparison of Local Nusselt Number for Steady and Pulsating Circular Jet at Reynolds Number of 16000, *European Journal of Scientific Research*, 29 (2009), 3, pp. 369-378
- [14] Haneda, Y., *et al.*, Enhancement of Impinging Jet Heat Transfer by Making Use of Mechano-Fluid Interactive Flow Oscillation, *International Journal of Heat Fluid flow*, 19 (1998), 2, pp. 115-124
- [15] Chaniotis, A. K., Poulidakos, D., Ventkos, Y., Dual Pulsating or Steady Slot Jet Cooling of a Constant Heat Flux Surface, *ASME Journal of Heat Transfer*, 125 (2003), 4, pp. 575-586
- [16] Bejera, R. C., Dutta, P., Srinivasan, K., Numerical Study of Interrupted Impinging Jets for Cooling of Electronics, *IEEE Transactions on Components and Packaging Technologies*, 30 (2007), 2, pp. 275-284
- [17] Poh, H. J., Kumar, K., Mujumdar, A. S., Heat Transfer from a Pulsed Laminar Impinging Jet, *International Communication for Heat & Mass Transfer*, 32 (2005), 10, pp. 1317-1324
- [18] Poh, H. J., Mujumdar, A. S., Heat Transfer from a Pulsed Turbulent Impinging Jet at Large Temperature Differences, *Proceedings, 5th Asia-Pacific Drying Conference*, Hong Kong, 2007, pp. 1171-1177
- [19] Fallen, M., Heat Transfer in a Pipe with Superimposed Pulsating Flow, *Heat and Mass Transfer*, 16 (1982), 2, pp. 89-99
- [20] Sheriff, H. S., Zumbunnen, D. A., Effect of Flow Pulsations on the Cooling Effectiveness of an Impinging Jet, *Journal of Heat Transfer*, 116 (1994), 4, pp. 886-895
- [21] Azevedo, L. F. A., Webb, B. W., Queiroz, M., Pulsed Air-jet Impingement Heat-Transfer, *Experimental Thermal and Fluid Science*, 8 (1994), 3, pp. 206-213
- [22] Mladin, E. C., Zumbunnen, D. A., Nonlinear Dynamics of Laminar Boundary Layers in Pulsatile Stagnation Flows, *Journal of Thermophysics and Heat Transfer*, 8 (1994), 32, pp. 514-523
- [23] Mladin, E. C., Zumbunnen, D. A., Alterations to Coherent Flow Structures and Heat Transfer Due to Pulsations in an Impinging Air-Jet, *International Journal of Thermal Science*, 39 (2000), 2, pp. 236-248
- [24] Vejrazka, J., Experimental Study of a Pulsating Round Impinging Jet, Ph. D. thesis, Institut National Polytechnique de Grenoble, Grenoble, France, 2002
- [25] Mladin, E. C., Zumbunnen, D. A., Dependence of Heat Transfer to a Pulsating Stagnation Flow on Pulse Characteristics, *Journal of Thermophysics and Heat Transfer*, 9 (1995), 1, pp. 181-192
- [26] Hofmann, H. M., *et al.*, Influence of a Pulsation on Heat Transfer and Flow Structure in Submerged Impinging Jets, *International Journal of Heat and Mass Transfer*, 50 (2007), 17-18, pp. 3638-3648
- [27] Wang, S. J., Mujumdar, A. S., A Comparative Study of Five Low Reynolds Number k - ϵ Models for Impingement Heat Transfer, *Applied Thermal Engineering*, 25 (2005), 1, pp. 31-44
- [28] Fujimoto, H., *et al.*, Numerical Simulation of Transient Cooling of a Hot Solid by an Impinging Free Surface Jet, *Numerical Heat Transfer, Part A: Applications*, 36 (1999), 8, pp. 767-780
- [29] Morris, G. K., Garimella, S. V., Fitzgerald, J. A., Flow-Field Prediction in Submerged and Confined Jet Impingement Using the Reynold Stress Model, *Journal of Electronic Packaging*, 121 (1999), 4, pp. 255-262
- [30] Shi, Y. L., Ray, M. B., Mujumdar, A. S., Computational Study of Impingement Heat Transfer under a Turbulent Slot Jet, *Industrial and Engineering Chemistry Research*, 41 (2001), 18, pp. 4643-4651
- [31] Behnia, M., *et al.*, Numerical Study of Turbulent Heat Transfer in Confined and Unconfined Impinging Jets, *International Journal of Heat and Fluid Flow*, 20 (1999), 1, pp. 1-9
- [32] Shi, Y. L., Ray, M. B., Mujumdar, A. S., Effect of Large Temperature Differences on Local Nusselt Number under Turbulent Slot Impingement Jet, *Drying Technology*, 20 (2002), 9, pp. 1803-1825